

Electron Density Measurement of MHD Combustion Plasmas with a Far-Infrared Laser

Nakamuta, Hironori

Department of Energy Conversion Engineering, Interdisciplinary Graduate School of Engineering Sciences, Kyushu University

Masuda, Mitsuharu

Department of Energy Conversion Engineering, Interdisciplinary Graduate School of Engineering Sciences, Kyushu University

Watanabe, Yukio

Department of Electrical Engineering, Faculty of Engineering, Kyushu University

Ikegami, Tomoaki

Department of Electrical Engineering, Faculty of Engineering, Kyushu University

他

<https://doi.org/10.15017/17681>

出版情報：九州大学大学院総合理工学報告. 9 (1), pp.29-36, 1987-07-25. 九州大学大学院総合理工学研究科

バージョン：

権利関係：

Electron Density Measurement of MHD Combustion Plasmas with a Far-Infrared Laser

Hironori NAKAMUTA*, Mitsuharu MASUDA**, Yukio WATANABE***
Tomoaki Ikegami***, and Masanori Akazaki**

(Received March 31, 1987)

The electron density is the most important parameter for the performance of an MHD power generator. The far-infrared laser has offered a powerful diagnostic tool for measuring this quantity. However, the effect of neutral gases should be made clear to improve accuracy. In the present paper, the variable wavelength far-infrared laser is used to solve this problem. In the electron density measurement with a Michelson interferometer, the definite fringe shift due to neutral gases in the flame is detected, and the effect of neutral gases, especially that of the rotational absorption by water molecules on the flame refractivity is quantitatively clarified. The measured electron density agrees very well with theoretical calculations.

1. Introduction

To clarify various phenomena associated with an MHD power generator, it is necessary to carry experiments with nonintrusive diagnostic methods. Especially, the electron density of a seeded combustion plasma is an important parameter for an MHD generator performance, and the experimental method to determine this accurately is needed to be developed. This parameter has been measured by electrostatic probes or RF probes. However, these intrusive probes inevitably disturb the flow field inside an MHD channel, and the obtained values are thought to have large errors¹⁾. The nonintrusive diagnostic method with a far-infrared (FIR) laser was proposed and tested.^{1,2)} In this method, the electron density was measured with the interferometry. In these works, the combustion plasma was obtained from a channel or a burner, the scale of which was small compared with a commercial MHD generation channel. These small scale experiments allowed using long wavelength lasers, because the laser beam was not attenuated significantly when the optical distance of a beam through a plasma was not long. For a large combustion plasma that will be encountered in a commercial size generator, the long wavelength laser may not be applied because of its large attenuation in the flame, and the short wavelength should be used. However, in the interferometric measurement of an electron density, the use of a short wavelength may result in the fringe shift caused by neutral gases in a flame, and this fringe shift may become comparable with or even larger than that due to electrons. Therefore, the effect of neutral gases should be made clear before applying this method to large scale channels.

The main purpose of the present research is to clarify this effect. Since this is expected to be dependent on laser wavelength, it is necessary to use the FIR laser with vari-

*Graduate Student, Department of Energy Conversion Engineering

**Department of Energy Conversion Engineering

***Department of Electrical Engineering

able wavelength. The present experiment uses a methanol laser, which is pumped optically by a CO₂ laser and is capable of lasing with wavelength of 118.8, 251.1 and 570.5 μm. In the electron density measurement with a Michelson interferometer, the definite fringe shift due to neutral gases in the flame is detected, and the effect of neutral gases, especially that of the rotational absorption by water molecules on the flame refractivity is quantitatively clarified. The measured electron density agrees very well with theoretical calculations.

2. Basic theory of FIR diagnostics

A laser beam with a wavelength λ is assumed to be transmitted through atmosphere. When a plasma with thickness L is generated across a beam path, the phase difference $\Delta\phi$ caused by this plasma is expressed as

$$\Delta\phi = 2\pi (\mu_a - \mu_p) L/\lambda \quad (1)$$

where μ_a and μ_p are the refractive indices of air and plasma respectively. If the laser beam is interfered with a reference beam which bypasses the plasma, the interference fringe shift ΔN due to plasma is

$$\Delta N = \Delta\phi / 2\pi = (\mu_a - \mu_p) L/\lambda \quad (2)$$

An MHD plasma is composed of electrons, ions and neutral gases, and the refractive index μ_p of which is given as

$$\mu_p - 1 = K_e n_e + K_i n_i + K_g n_g \quad (3)$$

where K_e , K_i and K_g are the specific refractivities and n_e , n_i and n_g are the number densities of electrons, ions and neutral gases respectively. The refractive index of air is

$$\mu_a - 1 = K_a n_a \quad (4)$$

where K_a and n_a are the specific refractivity and the number density of air. Under a typical MHD plasma condition ($n_e \approx 10^{20} \text{m}^{-3}$, $T \approx 2500 \text{K}$), the FIR laser frequency is much higher than the plasma frequency as well as the electron collision frequency for momentum transfer. The specific refractivity of electrons K_e is then expressed as³⁾

$$K_e = - (e^2 / 8 \pi^2 m_e \epsilon_0 c^2) \lambda^2 \quad (5)$$

where e is the electronic charge, m_e the electron mass, ϵ_0 the permittivity of free space and c the speed of light in vacuum.

Since $n_e \approx n_i \approx 10^{20} \text{m}^{-3}$, $n_g \approx 10^{24} \text{m}^{-3}$ and $K_i \approx K_g$ in an MHD plasma, the contribution of ions to μ_p is negligible, and the fringe shift per unit length of plasma is

$$\begin{aligned} \Delta N/L &= (\Delta N)_a/L - (\Delta N)_g/L - (\Delta N)_e/L \\ &= (K_a \bar{n}_a - K_g \bar{n}_g - K_e \bar{n}_e) / \lambda \end{aligned} \quad (6)$$

where \bar{n}_j ($j = a, g, e$) are the number densities averaged over a plasma length L . If the condition $(\Delta N)_e \gg [(\Delta N)_a - (\Delta N)_g]$ is satisfied, the value of $\Delta N/L$ depends only on the laser wavelength and electron density. However, when the laser wavelength is short, this condition may not be fulfilled. The detailed discussion on the validity of this condi-

tion will be given in the later section of this paper.

3. Experimental equipment

Figure 1 is the schematic diagram of the experimental equipment. The swirl stabilized spray combustor is operated on KOH seeded kerosene-oxygen with a thermal input of

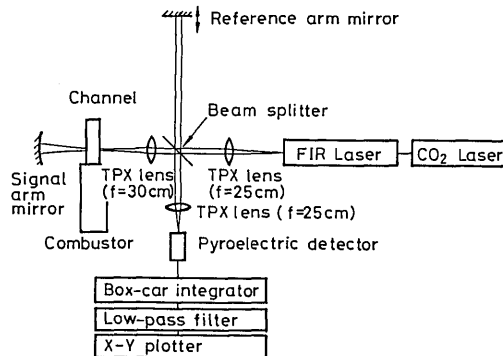


Fig. 1 Experimental equipment.

30kW, and discharges the flame into the channel under atmospheric pressure. The channel defines the path length of the laser beam through the plasma, and has a rectangular cross section of $20 \times 50 \text{ mm}^2$ with an estimated flame velocity of about 20 m/s. To transmit the laser beam along the wide dimension of the channel, the shorter side walls of the channel have $20 \times 20 \text{ mm}^2$ open holes at 20 mm downstream of the combustor exit. Since the main purpose of the present experiments is to develop the FIR laser diagnostics, the magnetic field is not applied. The combustor and the channel are made of metal, and no thermal insulation material is used to avoid the absorption and reemission of seed materials on the channel wall surface. This consideration makes it possible to measure accurately the fringe shift caused by the neutral components in the unseeded flame. The far-infrared laser is made of copper tube with 170 cm in length and 29 mm in internal diameter being filled with 10Pa methanol vapor, and is pumped by the CO₂ laser (Apollo 570, 50 W). Several wavelengths are obtained from this laser. The lines with wavelength of 118.8, 251.1 and $570.5 \mu\text{m}$ are strong among them, and the experimental results reported in this paper are obtained by these three lines. The intensity profiles of these lines are almost Gaussian in shape with the diameter for the $1/e^2$ intensity of about 5 mm at the channel center.

A Michelson interferometer is used to measure the electron density. The interferometer frame is made of glass ceramic to minimize the thermal expansion error, the linear expansion coefficient of which is very small and less than $1 \times 10^{-6} (1/\text{K})$. The beam splitter is a 0.05 mm thick Mylar film stretched over a brass frame to keep its surface flat when it is exposed to the radiation from the flame. The fringe shift is measured with the pyroelectric detector with a sensing area of 2 mm in diameter. Several polyethylene films are placed both on the signal arm and in front of the detector to reduce the thermal noise

from the flame. The detected signals are processed with the box-car integrator and the low-pass filter, and then recorded with the X-Y plotter. With these arrangements, it is possible to detect the displacement of the micrometer attached to the reference arm mirror with errors less than $\pm 2 \mu\text{m}$.

4. Experimental results and discussion

The experimental results of the fringe shift per unit length of plasma for the laser wavelength of 118.8, 251.1 and 570.5 μm are shown in **Fig. 2**, where K is the mass fraction

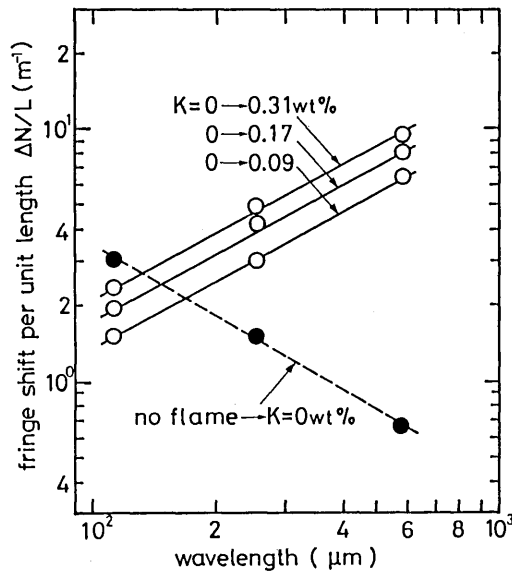


Fig. 2 Fringe shifts vs. laser wavelength.

of potassium seed and the plasma length $L/2$ is taken as the channel width (5 cm). In the measurement of the fringe shift at each wavelength, the readings of the micrometer attached to the reference arm mirror were recorded at the position of five adjacent fringe minima and were averaged. This procedure was repeated at conditions with no flame and with flame with the seeding fraction K being varied from 0 to 0.31wt%. The fringe shift was obtained by the difference of these micrometer readings between two of the conditions. The definite fringe shift is observed when the flame is turned on (no flame $\rightarrow K=0\text{wt}\%$). Since the seed deposited on the metal walls of the channel and combustor is cleaned at the beginning of every experiment, the obtained fringe shift is caused purely by neutral gases. This fringe shift has not been measured accurately so far, because this is usually small in the laboratory scale MHD channels and the seed material is deposited on their walls. The fringe shifts from the unseeded flame to the seeded flame are caused by electrons.

We shall first describe the fringe shift due to neutral gases. As shown by solid circles in **Fig. 2**, this fringe shift is inversely proportional to laser wavelength. Since the

density of neutral gases at each wavelength is constant under the present flame condition, this means that the specific refractivity of neutral gases does not depend on laser wavelength as indicated in Eq. (6). The flame refractivity ($\mu_f - 1$) is given by the difference between the refractivity of atmosphere ($\mu_a - 1$) and that corresponding to the measured fringe shift. Therefore, it is necessary to estimate μ_a to obtain μ_f . The following semi-empirical equation for millimeter and submillimeter electromagnetic waves is considered to calculate ($\mu_a - 1$)^{4,5)}.

$$(\mu_a - 1) \times 10^6 = 103.5 \frac{p_a}{T} + 86.26 \frac{p_w}{T} + \epsilon_{\text{rot}} \quad (7)$$

where T is the temperature (K), and p_a and p_w the partial pressures (mmHg) of dry air and water vapor respectively. The first term of the right-hand side of Eq. (7) comes from the elastic polarization of dry air, and the second term from that of water vapor. The third term denoted by ϵ_{rot} is the contribution of the rotational absorption by water molecules, and this is the only dispersive term. The value of ϵ_{rot} was calculated for each wavelength of the present FIR laser by using line absorption data,⁴⁾ and it was found that the variation of ($\mu_a - 1$) with wavelength was less than 10% because of the low water vapor pressure in the no flame condition (about 22 mmHg). The refractivity of a flame calculated with Eq. (7) and the experimental fringe shift of **Fig. 2** is $(35 \pm 25) \times 10^{-6}$.

To estimate this result theoretically, Eq. (7) is extended to the high temperature flame condition. The major components of the flame are CO_2 , H_2O , O_2 and N_2 , so that the first term of Eq. (7) is decomposed into terms for O_2 and N_2 , and also the CO_2 term is added. Using the data of Essen and Froome⁶⁾, Eq. (7) is rewritten as,

$$(\mu_f - 1) \times 10^6 = 95.69 \frac{p_{\text{O}}}{T} + 105.7 \frac{p_{\text{N}}}{T} + 86.26 \frac{p_w}{T} + 177.4 \frac{p_{\text{C}}}{T} + \epsilon_{\text{rot}} \quad (8)$$

where p_{O} , p_{N} and p_{C} are the partial pressures (mmHg) of oxygen, nitrogen and carbon dioxide respectively. To estimate ($\mu_f - 1$) with Eq. (8), the flame temperature T was measured by the line-reversal method and was found as $T = 2620\text{K}$. The values of p_{O} , p_{N} , p_w and p_{C} were obtained by the calculation with the chemical equilibrium code for combustion⁷⁾ for this measured temperature. Since the value of ϵ_{rot} in high temperature condition had not been reported, this term was calculated for $570.5 \mu\text{m}$ with the assumption of the rigid asymmetrical top rotor model for a water molecule.^{5,8)} The result is indicated in **Fig. 3**, where ϵ_{rot} normalized by its value at $T = 300\text{K}$ is plotted as a function of T . As shown in this figure, the value of ϵ_{rot} decreases rapidly with the increase in T , and $\epsilon_{\text{rot}} / \epsilon_{\text{rot}}(T = 300\text{K}) < 0.01$ for $T > 2600\text{K}$. While this calculation is for $570.5 \mu\text{m}$, ϵ_{rot} should also be small for the other wavelength because it contains Boltzmann factor and approaches zero with the increase in T . Although p_w is high in the present flame (about 260 mmHg), the value of ϵ_{rot} is found negligibly small compared with the other terms in the right-hand side of Eq. (8). Because that ϵ_{rot} is the only dispersive term in Eq. (8), the value of ($\mu_f - 1$) calculated by neglecting this term is independent of wavelength and 45×10^{-6} , which agrees reasonably well with the present experiment. Hubner and Jones measured the refractivity of the burner flame ($T = 1400 \sim 1600\text{K}$) with the single line HCN laser (wavelength $337 \mu\text{m}$).⁹⁾ They tried to explain their experimental results with Eq. (7). However, they used the value of ϵ_{rot} for $T = 300\text{K}$ and did not consider the variation of ϵ_{rot}

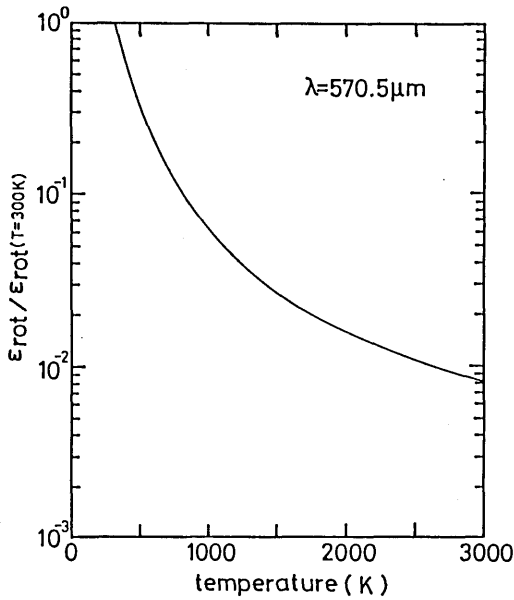


Fig. 3 Temperature dependence of the rotational absorption term of water molecules.

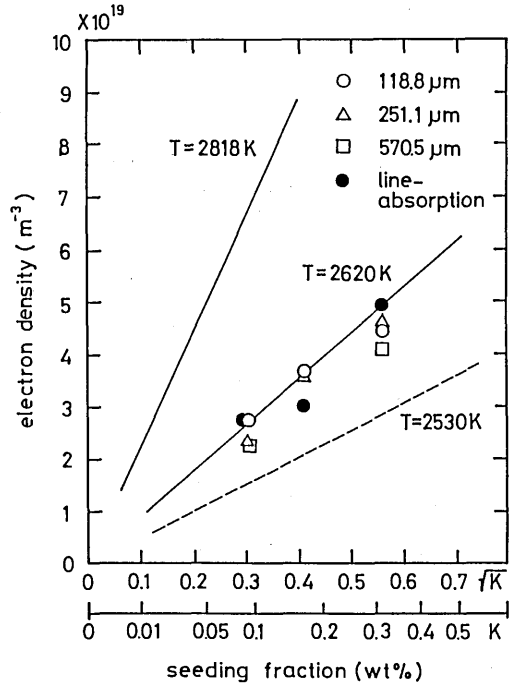


Fig. 4 Electron density vs. seeding fraction.

with temperature. This resulted in the large discrepancy between theory and experiments, and they suspected that Eq. (7) overestimated ϵ_{rot} . As shown in Fig. 3, $\epsilon_{rot} / \epsilon_{rot}(T=300K) < 0.03$ for their experiments and the present analysis also gives a satisfactory explanation to their results. To be added is the effect of the vibrational excitation of water molecules on ϵ_{rot} . The vibrational energies of the first and the second excitation levels are 0.19 and 0.39 eV above the ground level respectively.¹⁰⁾ This means that a part of water molecules may be vibrationally excited in the flame, and the rigid asymmetrical top rotor model may no longer be applicable. However, to neglect this effect seems justifiable since, as described above, the calculated refractivities agree well with experiments. Therefore, when the FIR laser interferometry is used under MHD conditions, the present result suggests that Eq. (8) can estimate the fringe shift due to neutral gases in the flame by neglecting the ϵ_{rot} term.

Since the fringe shift due to neutral gases is made clear in the present experiments, that for the seeded flame accurately determines the electron density. As shown in Fig. 2, the measured electron density is independent of the laser wavelength and is $2.5 \times 10^{19} \text{ m}^{-3}$ for $K=0.09 \text{ wt}\%$, $3.6 \times 10^{19} \text{ m}^{-3}$ for $K=0.17 \text{ wt}\%$ and $4.4 \times 10^{19} \text{ m}^{-3}$ for $K=0.31 \text{ wt}\%$.

Figure 4 shows the electron density as a function of the seeding fraction. The solid and broken lines are the electron density calculated with the chemical equilibrium code⁷⁾ with T as a parameter. According to the calculation, the adiabatic flame temperature was 2818K. The present results of the three laser wavelengths are found close to the theoretic-

cal electron density for the temperature of 2620K, which is the measured temperature with the line-reversal method. The broken line is the calculated flame temperature by taking into account the heat loss in the combustor estimated from the measured temperature increase of the cooling water. As shown in the figure, the experimental electron density is somewhat higher than this calculated value. The electron densities were also calculated from the seed atom density obtained with the potassium line-absorption method¹¹⁾ by assuming the Saha equilibrium. These are indicated by solid circles. These results agree very well with those from the FIR technique.

Since the electron density measured by the present FIR-method is averaged values along the laser beam path in the channel, these may be affected by the boundary layers developed along the channel walls. On the other hand, the temperature measured by the line-reversal is based on the wing-reversal technique and is regarded as that in the core flow. This means that the calculated electron density for $T = 2620\text{K}$ in **Fig. 4** also corresponds to its value in the core, and can be higher than the measured values. Therefore, the boundary layer thickness was estimated¹²⁾, and it was found that the effect of the boundary layer was about 8% of the measured values. The electron density corrected for this effect results in the better agreement with the theoretical calculations.

5. Conclusions

The methanol far-infrared laser with variable wavelength is constructed to measure the electron density of the MHD plasma obtained from the combustion of KOH seeded kerosene-oxygen. In the measurement with a Michelson interferometer, the fringe shift caused by the neutral gases in the flame is obtained with high degree of accuracy, and it is shown that this fringe shift can be explained quite well by extending the refractivity theory of standard atmosphere to the high temperature flame condition. Especially, the effect of the rotational absorption by water molecules on the refractivity is shown to be negligible under the flame condition. Because the fringe shift due to neutral gases is made clear in the present experiments, that for the seeded flame accurately determines the electron density. The measured electron density is found independent of the laser wavelength and agree very well with the results obtained from the potassium line-reversal and absorption methods. It is also shown that the measured electron density agrees with the calculated results for the temperature measured with the line-reversal method.

Acknowledgments

Authors are grateful to Mr. H. Chiwata, Mr. M. Yamakawa and Mr. T. Funatsu for their assistance in the experimental work. This work was partly supported by the Grant in Aid for Scientific Research, Ministry of Education, Science and Culture, Japan.

References

- 1) Self, S. A., Reigel, F. O., Clements, R. M. and James, R. K., "Electron Concentration Measurements in Combustion MHD Flows by Submillimeter Laser Interferometry", *Journal of Energy*, Vol. 1, No. 4, 1977, pp. 206-211.
- 2) Vasil'eva, I. A., Shumyatskii, B. Y. and Yundev, D. N., "Possibility of Measuring Electron Density and Electron Collision Frequency in Plasma Composed of Combustion Products using 337- μm Laser Interferometer", *High*

- Temperature, Vol. 13, 1975, pp. 1146-1150.
- 3) Heald, M. A. and Wharton, C. B., "Plasma Diagnostics with Microwaves", John Wiley & Sons Inc., 1965.
 - 4) Chamberlain, J. E., Findlay, F. D. and Gebbie, H. A., "Refractive Index of Air at 0.337-mm Wave-Length", Nature, Vol. 206, 1965, pp. 886-887.
 - 5) Zhevakin, S. A. and Naumov, A. P., "The Index of Refraction of Lower Atmosphere for Millimeter and Submillimeter Radiowaves. The Rotational Part of the Dielectric Permittivity of Atmospheric Water Vapor at Wavelength Greater than 10 Micrometers." Radio Engineering and Electronic Physics, Vol. 12, 1967, pp. 1067-1076.
 - 6) Essen, L. and Froome, K. D., "The Refractive Indices and Dielectric Constants of Air and its Principal Constituents at 24,000Mc/s", Proceedings of Physical Society, Vol. 64, 1951, pp. 1391-1398.
 - 7) Kutsuwada, T. and Honda, T., "Calculation of Thermodynamical and Electrical Properties of Combustion Products for MHD Generator", Bulletin of the Electrotechnical Laboratory, Vol. 32, 1968, pp. 520-542 (in Japanese).
 - 8) Hall, J. T., "Attenuation of Millimeter Wavelength Radiation by Gaseous Water", Applied Optics, Vol. 6, 1967, pp. 1391-1398.
 - 9) Hubner, G. and Jones, A. R., "Refractive Index of Flames in the Far Infrared", Journal of Physics D: Applied Physics, Vol. 6, 1973, pp. 774-778.
 - 10) Benedict, W. S., Pollack, M. A. and Tomlinson, W. J., "The Water-Vapor Laser", IEEE Journal of Quantum Electronics, Vol. QE-5, 1969, pp. 108-124.
 - 11) Kirkbright, G. F. and Sargent, M., "Atomic Absorption and Fluorescence Spectroscopy", Academic Press, London, 1974, pp. 47-63.
 - 12) Schlichting, H., "Boundary-Layer Theory", 7th ed. McGraw-Hill Co., 1979, pp. 303-309.